Received: 5 August 2020 | Revised: 14 March 2021 | Accepted: 31 May 2021

DOI: 10.1002/cyto.a.24474

OMIP

MIFlowCyt

ISAC CYTOMETRY Journal of Quantitative Cell Science PART A

OMIP 076: High-dimensional immunophenotyping of murine T-cell, B-cell, and antibody secreting cell subsets

Kyle T. Mincham | Jacob D. Young | Deborah H. Strickland

Telethon Kids Institute, University of Western Australia, Nedlands, Western Australia, Australia

Correspondence
Deborah H. Strickland, Northern Entrance, Perth Children's Hospital, 15 Hospital Avenue, Nedlands, Western Australia, Australia.
Email: deb.strickland@telethonkids.org.au

Funding information
Telethon Kids Institute

KEYWORDS: antibody secreting cell, B cell, high-dimensional flow cytometry, lymphocyte, splenocytes, T cell

1 | PURPOSE AND APPROPRIATE SAMPLE TYPES

This 19-parameter, 18-color flow cytometry panel was designed and optimized to enable the comprehensive and simultaneous immunophenotyping of distinct T-cell, B-cell, and antibody secreting cell (ASC) subsets within murine tissues (Table 1). Cellular populations identified by using this OMIP include two major subsets of B-cells (memory and activated), two ASC subsets (plasma cells and plasmablasts), and seven major subsets of $CD4^+$ T-cells (naïve, central memory, effector memory, helper, regulatory, follicular helper, and follicular regulatory). Staining was performed on freshly isolated splenocytes from 21-day-old BALB/c mice, however, due to the omission of mouse strain-specific markers, this OMIP can be implemented across a range of murine models where in-depth immunophenotyping of the diverse repertoire of T-cell, B-cell, and ASC populations is required.

2 | BACKGROUND

There is now considerable evidence demonstrating that both prenatal and postnatal exposure to particular classes of microbial stimuli can provide beneficial signals during early life immune development, resulting in the protection against future inflammatory disease [1-3]. The principal target of this beneficial immunostimulation appears to be the innate immune system [4, 5], and the mechanisms driving protection underlay the paradigm of innate immune training, whereby certain classes of microbial stimuli can alter the functional state of innate immune cells, leading to the optimization of immunocompetence [6]. Immune training focuses on the phenotypic and transcriptional profiles of several prototypical innate populations [6, 7], however, the characterization of downstream adaptive responses associated with protection via innate immune training are of critical importance for understanding disease pathogenesis, and the potential for therapeutic mitigation. Due to this gap in our current understanding, the broader protective mechanisms remain incompletely understood. To address this requirement, we have developed and optimized a novel 19-parameter flow cytometry panel to comprehensively and simultaneously characterize distinct T-cell, B-cell, and ASC subsets localized within tissues of BALB/c mice in response to immune training during early life.

The developmental phase of this flow cytometry panel involved the prioritization of T-cell, B-cell, and ASC subsets central to the maintenance of immunological homeostasis, as based on the current literature and forerunner studies. As such, a degree of emphasis was placed on effector, regulatory, and memory subsets within T-cell and B-cell populations. In regard to T-cells, the conversion of peripheral naïve $CD4^+$ T-cells to effector T (Teff) cells is denoted by upregulation of the activation marker CD25, while concomitant upregulation of both CD25 and intracellular Foxp3 expression is essential for the peripheral induction of regulatory T-cells (Treg) [8], a process previously recognized in the protection against allergic airways inflammation following microbial-derived immunomodulation [9, 10]. Furthermore, the expression of CD44 on Treg has been implicated in promoting enhanced function [11, 12], while inducible costimulator $(ICOS)^+$ Tregs are recognized to have superior suppressive capacity and interleukin (IL)-10 production compared to $ICOS^-$ Tregs [13, 14]. Following activation and contraction, $CD4^+$ T-cells transition toward a

memory phenotype via the gradual upregulation of CD44 expression in parallel with transient expression of CD62L, driving the establishment of a dynamic repository of central memory (T_{CM}) and effector memory (T_{EM}) T-cells [15-17]. In addition to establishing peripheral memory, activated $CD4^+$ T-cells have the capacity to upregulate extracellular expression of CXCR5, ICOS, and programmed cell death protein 1 (PD-1) [18, 19], resulting in the generation of a highly specialized population of T follicular helper (T_{FH}) cells required for the formation of germinal centers within secondary lymphoid organs, while also providing crucial survival signals to support high-affinity B-cells during affinity maturation and proliferation [20, 21]. A separate subset of thymic-derived cells that share homology with the T_{FH} phenotype in addition to Foxp3 and bimodal CD25 expression, termed follicular regulatory T (T_{FR}) cells, have also been identified, however, this subset has been attributed to the inhibition of T_{FH} activity and subsequent generation of humoral immunity [22, 23]. The immunophenotypic characterization of B-cell and ASC subsets for this OMIP was centered around the classic expression of CD19 and B220. To maximize the capacity of a 5-laser BD LSRFortessa™, CD19 (B-cell and ASC subsets) and CD4 (T-cell) antibodies were conjugated to the same fluorochrome, since co-expression is essentially absent in single-cell analysis. Within secondary lymphoid tissues, the antigen-specific activation of B-cells involves the constitutive upregulation of major histocompatibility complex class-II (MHC class II; mouse I-A/I-E) and CD80 expression, in conjunction with the membrane-bound expression of both immunoglobulin (Ig) M and IgD [24-26]. Following antigen-specific activation, B-cells upregulate Synd-1 expression and differentiate into the two major classes of ASC; the rapidly produced and short-lived plasmablasts and the short-lived peripheral plasma cells, both of which have the capacity to secrete IgM [27-30]. A major difference between these two antibody-secreting subsets, however, is the absence of classic mature B-cell markers CD19, B220, and MHC-II on plasma cells [28, 31]. The eventual transition of B-cells toward a memory phenotype results in the loss of Synd-1 expression with parallel upregulation of programmed cell death protein 1 ligand 2 (PD-L2), generating a long-lived secondary lymphoid population expressing IgM $+/-$ IgD that can rapidly differentiate into ASC upon re-stimulation [32-36].

Panel optimization was performed on a BD LSRFortessa™, with all fluorochrome-conjugated antibodies (Table 2) titrated during the optimization phase (Figure S1). Prior to multicolor extracellular staining, splenocytes were incubated in Fc Block™ (Purified recombinant CD16/32) to inhibit non-antigen-specific binding of fluorochrome-conjugated antibodies to the nonpolymorphic epitope of FcγIII (CD16) and FcγII (CD32) receptors expressed on multiple myeloid populations and B-cells. A representative gating strategy to delineate the T-cell, B-cell, and ASC subsets described above is detailed in Figure 1. Briefly, splenocytes were first gated on side-scatter (SSC) and forward-scatter (FSC) parameters (Figure 1A) to

TABLE 1 Summary table

Purpose	Comprehensive immunophenotyping of T-cell, B-cell, and ASC subsets
Species	Mouse
Cell types	Murine tissues containing lymphocyte populations
Cross-reference	OMIP-031, OMIP-032, OMIP-054, OMIP-061

TABLE 2 Reagents used for OMIP

Specificity	Fluorochrome	Clone	Purpose
PD-L2 (CD273)	BUV395	TY25	Memory B-cells
IgD	BUV496	AMS 9.1	Activated/memory B-cells
CD44	BUV737	IM7	T-cell subsets
ICOS (CD278)	BV421	7E.17G9	T Follicular helper/Treg
PD-1 (CD279)	BV480	J43	T Follicular helper cells
Live/Dead	FVS575	N/A	Viable cells
CD80	BV650	16-10A1	Activated B-cells
IgM	BV711	R6.60.2	B-cell/ASC subsets
CD4	BV786	RM4-5	$CD4^+$ T-cells
CD19	BV786	1D3	B-cell subsets
Synd-1 (CD138)	BB515	281-2	Plasmablasts/Plasma cells
TCRβ	BB700	H57-597	Pan T-cells
Foxp3	PE	FJK-16s	Regulatory T-cells
B220 (CD45R)	PE-CF594	RA3-6B2	B-cell subsets
CD25	PE-Cy5	PC61	Activated T-cells
CXCR5 (CD185)	PE-Cy7	2G8	T Follicular helper cells
MHC class II (I-A/I-E)	AF647	M5/114.15.2	B-cell subsets
CD62L	APC-R700	MEL-14	T-cell subsets
CD45	APC-Cy7	30-F11	Pan leukocyte

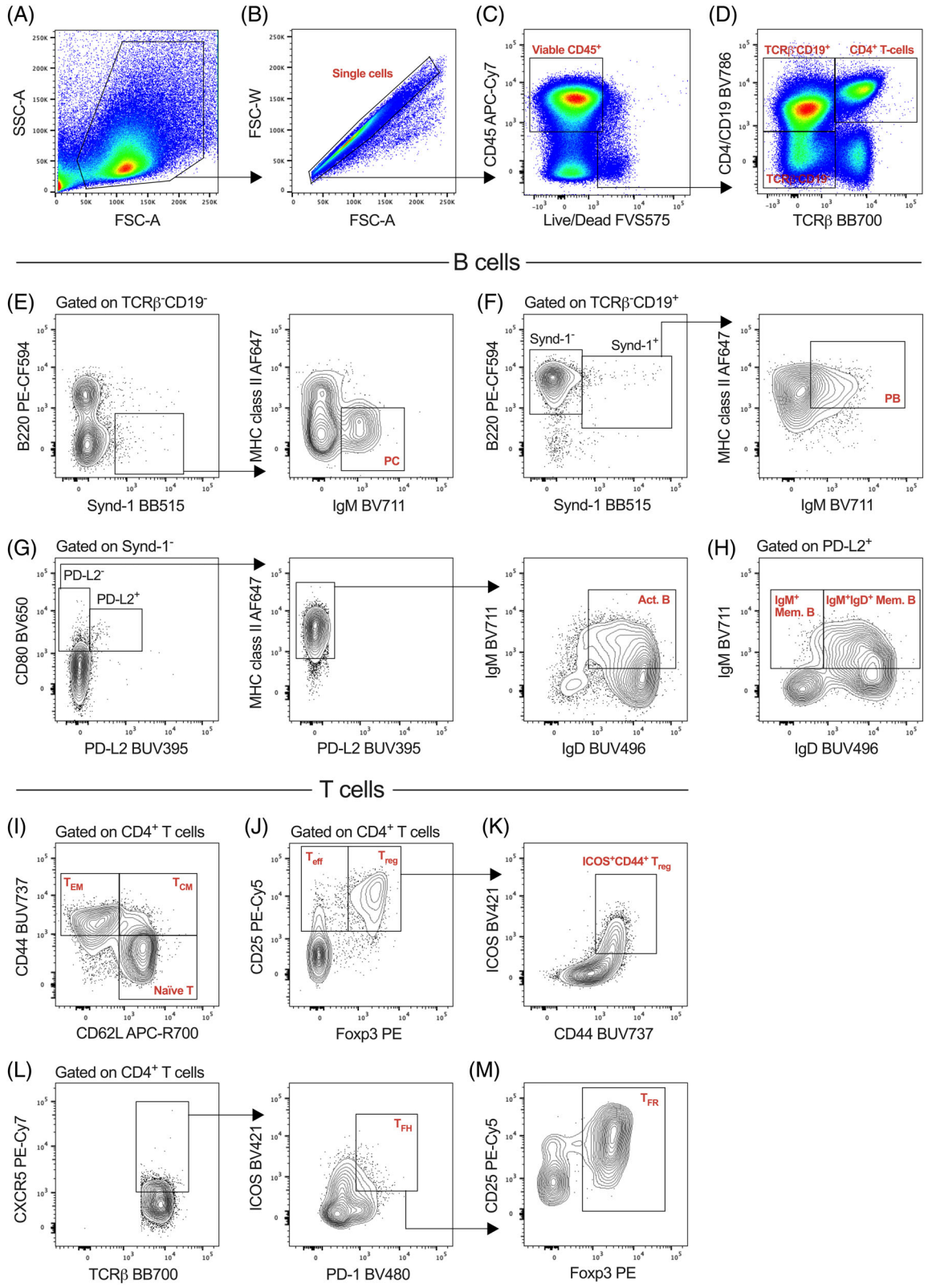

FIGURE 1 Overview of 19-parameter gating strategy developed for the characterization of T-cell, B-cell, and ASC subsets within freshly isolated splenocytes from 21-day-old BALB/c mice. 1×10^6 splenocytes were incubated in Fc Block™, followed by fixable viability stain (FVS) and a 17-parameter extracellular antibody cocktail containing 10% brilliant stain buffer plus (BD biosciences). Intracellular staining was performed following fixation-permeabilization of extracellular stained splenocytes. Data were acquired on a BD LSRFortessa™ (BD Biosciences). (A–C) Removal of cellular debris, doublets, nonviable cells and stromal cells. (D) Primary delineation of $TCR\beta^{-}CD19^{+}$, $TCR\beta^{+}CD4^{+}$, and $TCR\beta^{-}CD4/CD19^{-}$ cells. (E–M) Characterization of (E) plasma cells, (F) plasmablasts, (G) activated B-cells, (H) memory B-cells, (I) naïve, effector memory and central memory T-cells, (J) effector and regulatory T-cells, (K) $ICOS^{+}CD44^{+}$ Treg, (L) T follicular helper cells, and (M) follicular regulatory T-cells. All plots are representative of individual samples. Manual gating was determined using fluorescence minus one (FMO) controls where necessary (Figure S4) [Color figure can be viewed at wileyonlinelibrary.com]

remove sample debris, followed by single-cell gating (Figure 1B) to remove doublets. Gating was then performed on viable CD45$^+$ cells (Figure 1C) to remove dead/dying cells and stromal cells from the analysis. The primary T-cell/B-cell/ASC separation involved delineation of TCRβ and CD4/CD19 expression (Figure 1D). Double positive cells were classified as CD4$^+$ T-cells, as CD19$^+$ B-cells and ASC subsets will be present within the TCRβ$^-$ population (Figure 1D) due to the absence of TCRβ/CD19 co-expression (Figure S2A). An additional TCRβ$^-$CD4/CD19$^-$ gate was included to enable the characterization of B220$^-$Synd-1$^+$MHC class II$^-$IgM$^+$ plasma cells (PC; Figure 1E). CD19$^+$ B-cells and ASC subsets were then defined as B220$^{lo/+}$Synd-1$^+$MHC class II$^+$IgM$^+$ plasmablasts (PB; Figure 1F), B220$^+$Synd-1$^-$CD80$^+$PD-L2$^-$MHC class II$^+$IgM$^+$IgD$^+$ activated B-cells (Figure 1G) and B220$^+$Synd-1$^-$CD80$^+$PD-L2$^+$IgM$^+$IgD$^{+/-}$ memory B-cells (Figure 1H). CD4$^+$ T-cells were defined as CD62L$^+$CD44$^{lo/-}$ naïve T-cells (Figure 1I), CD62L$^+$CD44^{hi} T_{CM} (Figure 1I), CD62L$^-$CD44^{hi} T_{EM} (Figure 1I), CD25$^+$Foxp3$^-$ Teff (Figure 1J), CD25$^+$Foxp3$^+$ Treg (Figure 1J) ICOS$^+$CD44$^+$ Treg (Figure 1K), CXCR5$^+$ICOS$^+$PD-1$^+$ T_{FH} (Figure 1L), and CXCR5$^+$ICOS$^+$PD-1$^+$CD25$^{+/-}$Foxp3$^+$ T_{FR} (Figure 1M).

To perform high-dimensional analysis on 21-day-old naïve splenocytes, viable CD45$^+$ cells (Figure 1C) underwent high-resolution FlowSOM clustering to define cell populations, followed by metaclustering for visualization with Uniform Manifold Approximation and Projection (UMAP) [37] using the Cytometry Data Analysis Tool (CATALYST) pipeline [38, 39]. Primary unsupervised analysis was performed to identify CD4$^+$ T-cell and B-cell/ASC clusters based on extracellular receptor co-expression (Figure S3A). CD4$^+$ T-cell (Figure S3B), and B-cell/ASC (Figure S3C) clusters were then isolated for secondary subset analysis.

3 | SIMILARITIES TO OTHER OMIPS

The OMIP described here shares a small degree of marker similarity (TCRβ, CD4, CD44, CD62L, PD-1, CD19, B220) with OMIP-031 [40], OMIP-032 [41], and OMIP-061 [42], which are focused on immunologic checkpoint expression on murine T-cell subsets, the characterization of innate and adaptive populations within the murine mammary gland and murine antigen-presenting cells, respectively. While both OMIP-031 and OMIP-032 characterize TCRβ$^+$CD4$^+$ effector and memory T-cell subsets based on a combination of CD44 and/or CD62L expression, OMIP-032 employs an additional CD19$^+$ gate to delineate B-cells. OMIP-061 utilized B220 to identify B-cells. A distinct difference between these OMIPs and the OMIP described here is that our panel was developed for the sole purpose of comprehensively immunophenotyping T-cell, B-cell, and ASC subsets simultaneously, and we therefore include an additional 12 markers to allow the characterization of two major B-cell, two ASC and seven major T-cell populations within a single sample. The OMIP described here also exhibits minor overlap with OMIP-054 [43], however, our panel was developed to maximize the potential of a 5-laser BD LSRFortessa™ in facilities without the capacity to perform mass cytometry.

ACKNOWLEDGMENTS

The authors would like to thank Steven Roberts and Dr. Andrew Lim of BD Biosciences (Australia) for their valuable advice during the initial design of this OMIP.

AUTHOR CONTRIBUTIONS

Kyle Mincham: Conceptualization; data curation; formal analysis; funding acquisition; investigation; methodology; validation; visualization; writing-original draft; writing-review & editing. **Jacob Young:** Data curation; formal analysis; investigation; validation; writing-original draft. **Deborah Strickland:** Conceptualization; formal analysis; funding acquisition; investigation; methodology; project administration; writing-original draft; writing-review & editing.

CONFLICT OF INTEREST

The authors declare no conflict of interest exists.

ORCID

Kyle T. Mincham https://orcid.org/0000-0003-4419-7258

REFERENCES

1. Gollwitzer ES, Marsland BJ. Impact of early-life exposures on immune maturation and susceptibility to disease. Trends Immunol. 2015;36:684–96.
2. von Mutius E, Vercelli D. Farm living: effects on childhood asthma and allergy. Nat Rev Immunol. 2010;10:861–8.
3. Ober C, Sperling AI, von Mutius E, Vercelli D. Immune development and environment: lessons from Amish and Hutterite children. Curr Opin Immunol. 2017;48:51–60.
4. Schuijs MJ, Willart MA, Vergote K, Gras D, Deswarte K, Ege MJ, et al. Farm dust and endotoxin protect against allergy through A20 induction in lung epithelial cells. Science. 2015;349:1106–10.
5. Holt PG, Sly PD. Environmental microbial exposure and protection against asthma. N Engl J Med. 2015;373:2576–8.
6. Netea MG, Domínguez-Andrés J, Barreiro LB, Chavakis T, Divangahi M, Fuchs E, et al. Defining trained immunity and its role in health and disease. Nat Rev Immunol. 2020;20:375–88.
7. Mincham KT, Jones AC, Bodinier M, Scott NM, Lauzon-Joset J-F, Stumbles PA, et al. Transplacental innate immune training via maternal microbial exposure: role of XBP1-ERN1 Axis in dendritic cell precursor programming. Front Immunol. 2020;11:601494.
8. Chen W, Jin W, Hardegen N, Lei KJ, Li L, Marinos N, et al. Conversion of peripheral CD4 + CD25- naive T cells to CD4 + CD25+ regulatory T cells by TGF-β induction of transcription factor Foxp3. J Exp Med. 2003;198:1875–86.
9. Mincham KT, Scott NM, Lauzon-Joset JF, Leffler J, Larcombe AN, Stumbles PA, et al. Transplacental immune modulation with a bacterial-derived agent protects against allergic airway inflammation. J Clin Invest. 2018;128:4856–69.
10. Strickland DH, Judd S, Thomas JA, Larcombe AN, Sly PD, Holt PG. Boosting airway T-regulatory cells by gastrointestinal stimulation as a strategy for asthma control. Mucosal Immunol. 2011;4:43–52.
11. Bollyky PL, Falk BA, Long SA, Preisinger A, Braun KR, Wu RP, et al. CD44 costimulation promotes FoxP3+ regulatory T cell persistence and function via production of IL-2, IL-10, and TGF-beta. J Immunol. 2009;183:2232–41.
12. Firan M, Dhillon S, Estess P, Siegelman MH. Suppressor activity and potency among regulatory T cells is discriminated by functionally active CD44. Blood. 2006;107:619–27.
13. Vocanson M, Rozieres A, Hennino A, Poyet G, Gaillard V, Renaudineau S, et al. Inducible costimulator (ICOS) is a marker for

highly suppressive antigen-specific T cells sharing features of TH17/TH1 and regulatory T cells. J Allergy Clin Immunol. 2010;126:280–9.e7.
14. Redpath SA, van der Werf N, Cervera AM, MacDonald AS, Gray D, Maizels RM, et al. ICOS controls Foxp3(+) regulatory T-cell expansion, maintenance and IL-10 production during helminth infection. Eur J Immunol. 2013;43:705–15.
15. Sallusto F, Lenig D, Förster R, Lipp M, Lanzavecchia A. Two subsets of memory T lymphocytes with distinct homing potentials and effector functions. Nature. 1999;401:708–12.
16. Lanzavecchia A, Sallusto F. Understanding the generation and function of memory T cell subsets. Curr Opin Immunol. 2005;17:326–32.
17. Baaten BJ, Li CR, Deiro MF, Lin MM, Linton PJ, Bradley LM. CD44 regulates survival and memory development in Th1 cells. Immunity. 2010;32:104–15.
18. Choi YS, Kageyama R, Eto D, Escobar TC, Johnston RJ, Monticelli L, et al. ICOS receptor instructs T follicular helper cell versus effector cell differentiation via induction of the transcriptional repressor Bcl6. Immunity. 2011;34:932–46.
19. Schaerli P, Willimann K, Lang AB, Lipp M, Loetscher P, Moser B. CXC chemokine receptor 5 expression defines follicular homing T cells with B cell helper function. J Exp Med. 2000;192:1553–62.
20. Good-Jacobson KL, Szumilas CG, Chen L, Sharpe AH, Tomayko MM, Shlomchik MJ. PD-1 regulates germinal center B cell survival and the formation and affinity of long-lived plasma cells. Nat Immunol. 2010;11:535–42.
21. Crotty S. T follicular helper cell differentiation, function, and roles in disease. Immunity. 2014;41:529–42.
22. Linterman MA, Pierson W, Lee SK, Kallies A, Kawamoto S, Rayner TF, et al. Foxp3+ follicular regulatory T cells control the germinal center response. Nat Med. 2011;17:975–82.
23. Wing JB, Kitagawa Y, Locci M, Hume H, Tay C, Morita T, et al. A distinct subpopulation of CD25- T-follicular regulatory cells localizes in the germinal centers. Proc Natl Acad Sci U S A. 2017;114:E6400–E9.
24. Lankar D, Vincent-Schneider H, Briken V, Yokozeki T, Raposo G, Bonnerot C. Dynamics of major histocompatibility complex class II compartments during B cell receptor-mediated cell activation. J Exp Med. 2002;195:461–72.
25. Borriello F, Sethna MP, Boyd SD, Schweitzer AN, Tivol EA, Jacoby D, et al. B7-1 and B7-2 have overlapping, critical roles in immunoglobulin class switching and germinal center formation. Immunity. 1997;6:303–13.
26. Maity PC, Blount A, Jumaa H, Ronneberger O, Lillemeier BF, Reth M. B cell antigen receptors of the IgM and IgD classes are clustered in different protein islands that are altered during B cell activation. Sci Signal. 2015;8:ra93.
27. McHeyzer-Williams MG, McLean MJ, Lalor PA, Nossal GJ. Antigen-driven B cell differentiation in vivo. J Exp Med. 1993;178:295–307.
28. Kallies A, Hasbold J, Tarlinton DM, Dietrich W, Corcoran LM, Hodgkin PD, et al. Plasma cell ontogeny defined by quantitative changes in blimp-1 expression. J Exp Med. 2004;200:967–77.
29. Racine R, McLaughlin M, Jones DD, Wittmer ST, MacNamara KC, Woodland DL, et al. IgM production by bone marrow plasmablasts contributes to long-term protection against intracellular bacterial infection. J Immunol. 2011;186:1011–21.
30. Blanc P, Moro-Sibilot L, Barthly L, Jagot F, This S, de Bernard S, et al. Mature IgM-expressing plasma cells sense antigen and develop competence for cytokine production upon antigenic challenge. Nat Commun. 2016;7:13600.
31. Nutt SL, Hodgkin PD, Tarlinton DM, Corcoran LM. The generation of antibody-secreting plasma cells. Nat Rev Immunol. 2015;15:160–71.
32. Tomayko MM, Steinel NC, Anderson SM, Shlomchik MJ. Cutting edge: hierarchy of maturity of murine memory B cell subsets. J Immunol. 2010;185:7146–50.
33. Zuccarino-Catania GV, Sadanand S, Weisel FJ, Tomayko MM, Meng H, Kleinstein SH, et al. CD80 and PD-L2 define functionally distinct memory B cell subsets that are independent of antibody isotype. Nat Immunol. 2014;15:631–7.
34. McHeyzer-Williams LJ, McHeyzer-Williams MG. Antigen-specific memory B cell development. Annu Rev Immunol. 2005;23:487–513.
35. Dogan I, Bertocci B, Vilmont V, Delbos F, Mégret J, Storck S, et al. Multiple layers of B cell memory with different effector functions. Nat Immunol. 2009;10:1292–9.
36. Reynaud C-A, Descatoire M, Dogan I, Huetz F, Weller S, Weill J-C. IgM memory B cells: a mouse/human paradox. Cell Mol Life Sci. 2012;69:1625–34.
37. Becht E, McInnes L, Healy J, Dutertre C-A, Kwok IWH, Ng LG, et al. Dimensionality reduction for visualizing single-cell data using UMAP. Nat Biotechnol. 2019;37:38–44.
38. Crowell HL, Zanotelli VRT, Chevrier S, Robinson MD. CATALYST: Cytometry dATa anALYSis Tools 2020 https://github.com/HelenaLC/CATALYST.
39. Nowicka M, Krieg C, Crowell H, Weber L, Hartmann F, Guglietta S, et al. CyTOF workflow: differential discovery in high-throughput high-dimensional cytometry datasets. F1000Research. 2019;6:748.
40. Nemoto S, Mailloux AW, Kroeger J, Mulé JJ. OMIP-031: immunologic checkpoint expression on murine effector and memory T-cell subsets. Cytometry A. 2016;89:427–9.
41. Unsworth A, Anderson R, Haynes N, Britt K. OMIP-032: two multicolor immunophenotyping panels for assessing the innate and adaptive immune cells in the mouse mammary gland. Cytometry A. 2016;89:527–30.
42. DiPiazza AT, Hill JP, Graham BS, Ruckwardt TJ. OMIP-061: 20-color flow cytometry panel for high-dimensional characterization of murine antigen-presenting cells. Cytometry A. 2019;95:1226–30.
43. Dusoswa SA, Verhoeff J, Garcia-Vallejo JJ. OMIP-054: broad immune phenotyping of innate and adaptive leukocytes in the brain, spleen, and bone marrow of an orthotopic murine glioblastoma model by mass cytometry. Cytometry A. 2019;95:422–6.

SUPPORTING INFORMATION

Additional supporting information may be found online in the Supporting Information section at the end of this article.

How to cite this article: Mincham KT, Young JD, Strickland DH. OMIP 076: High-dimensional immunophenotyping of murine T-cell, B-cell, and antibody secreting cell subsets. Cytometry. 2021;99:888–892. https://doi.org/10.1002/cyto.a.24474